

# Quantitative Image Analysis of Protein Translocation using our High-Content Imagers and YT-SOFTWARE®

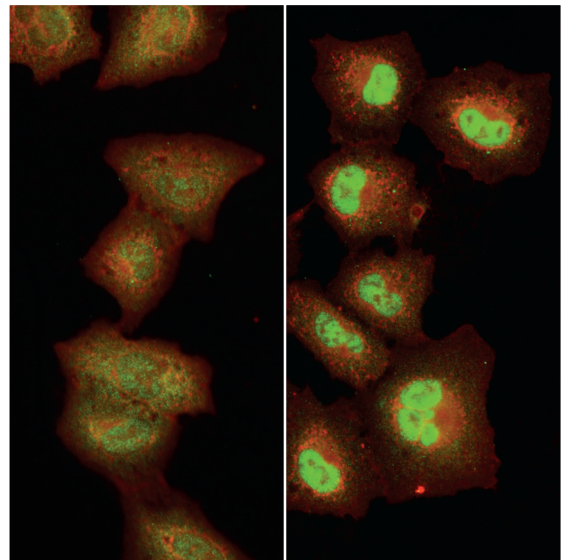
Willms A<sup>1</sup>, Aleks Guledani<sup>1</sup>, Kollenda S<sup>1</sup>, Stoehr M<sup>1</sup>, Werdelmann B<sup>1</sup>, Trauzold A<sup>2</sup>, Sebens S<sup>2</sup>, Geisen R<sup>1</sup> & Pirsch M<sup>1</sup>

<sup>1</sup>SYNENTEC GmbH, Elmshorn, Germany

<sup>2</sup>Institute for Experimental Cancer Research, CAU + UKSH Kiel, Germany

## ABSTRACT

Protein translocation between the cytosol and nucleus represents a fundamental process to maintain cellular functions. Therefore, the development of easy and fast methods to visualize and quantify protein translocation is important in various scientific fields. A commonly used method to analyze the localization of proteins in the cell is immunofluorescence staining. Performing immunofluorescence stainings presents challenges, due to complex protocols that demand a considerable amount of hands-on time. Moreover, depending on the microscope used, imaging can be time-intensive and image analysis often requires additional software. To address these challenges and enhance the accessibility of a translocation assay based on immunofluorescence stainings, we have developed and implemented a new image analysis tool in our YT-SOFTWARE®. This advancement enables imaging and image analysis within the same software platform. Moreover, our automated imagers NYONE® and CELLAVISTA® facilitate high-content screening using 4K resolution. Here, we performed translocation assays of two proteins, STAT3 and NF-κB. We induced protein trafficking by the cytokines IL-6/IL-6Rα and TNF-α in A549 and HT29 cancer cells and performed immunofluorescence stainings afterward. Stainings were imaged and analyzed using NYONE® or CELLAVISTA®, and the new image analysis application **Translocation (1F)** of YT-SOFTWARE®. The fluorescence signal in the nucleus clearly increased after treatment. In line with these results, image quantification confirmed the movement of STAT3 and NF-κB referred to the automatically calculated nucleus/cytoplasmic *translocation ratio*. Altogether, we developed an easy-to-use and fast tool to analyze protein translocation based on immunofluorescence stainings.



KEYWORDS: TRANSLOCATION, IMMUNOFLUORESCENCE STAINING, HIGH-CONTENT SCREENING, HIGH-THROUGHPUT SCREENING, SIGNAL TRANSDUCTION

## Benefits of SYNENTEC's Translocation Assay

- All in one software platform: imaging, image analysis and calculation of the *translocation ratio*.
- No slides required: IF-staining and imaging in microplates enable high throughput.
- Easy handling and suitable for automation systems.
- Automated and fast imaging of multiple samples with minimal hands-on time.

## INTRODUCTION

A fundamental cellular process is the translocation of proteins, referring to the movement of proteins from one intracellular compartment to another. Protein translocation is critical for many cellular processes, such as signal transduction, protein synthesis, and cell division. Therefore, it is not surprising that its perturbations can lead to e.g., neurodegenerative [1] and metabolic [2] diseases, as well as cancer [3]. Although the majority of proteins are synthesized in the cytoplasm, they need to be transported to different cellular compartments such as the nucleus, mitochondria, endoplasmic reticulum, Golgi apparatus or lysosomes to perform their functions. An important example is the translocation of transcription factors from the cytoplasm to the nucleus after activation by external or internal stimuli. One method to study protein translocation is

classical microscopy using confocal or other imaging techniques. This method is often time-consuming limiting its suitability for high-throughput screening. Moreover, quantitative analysis of the images often requires additional software with several steps to get results. Thus, training new users is time- and labor-intensive. The other option are biochemical methods like Western blots of cytoplasmatic *versus* nuclear extracts. However, they cannot provide information on individual cells or subpopulations. Hence, we aimed to establish a straightforward, and fast microscopy-based application to visualize and quantify protein translocation using SYNENTEC's automated imager and YT-SOFTWARE®. To develop and test the new **Translocation (1F)** application, we monitored the movement of two well-studied proteins between

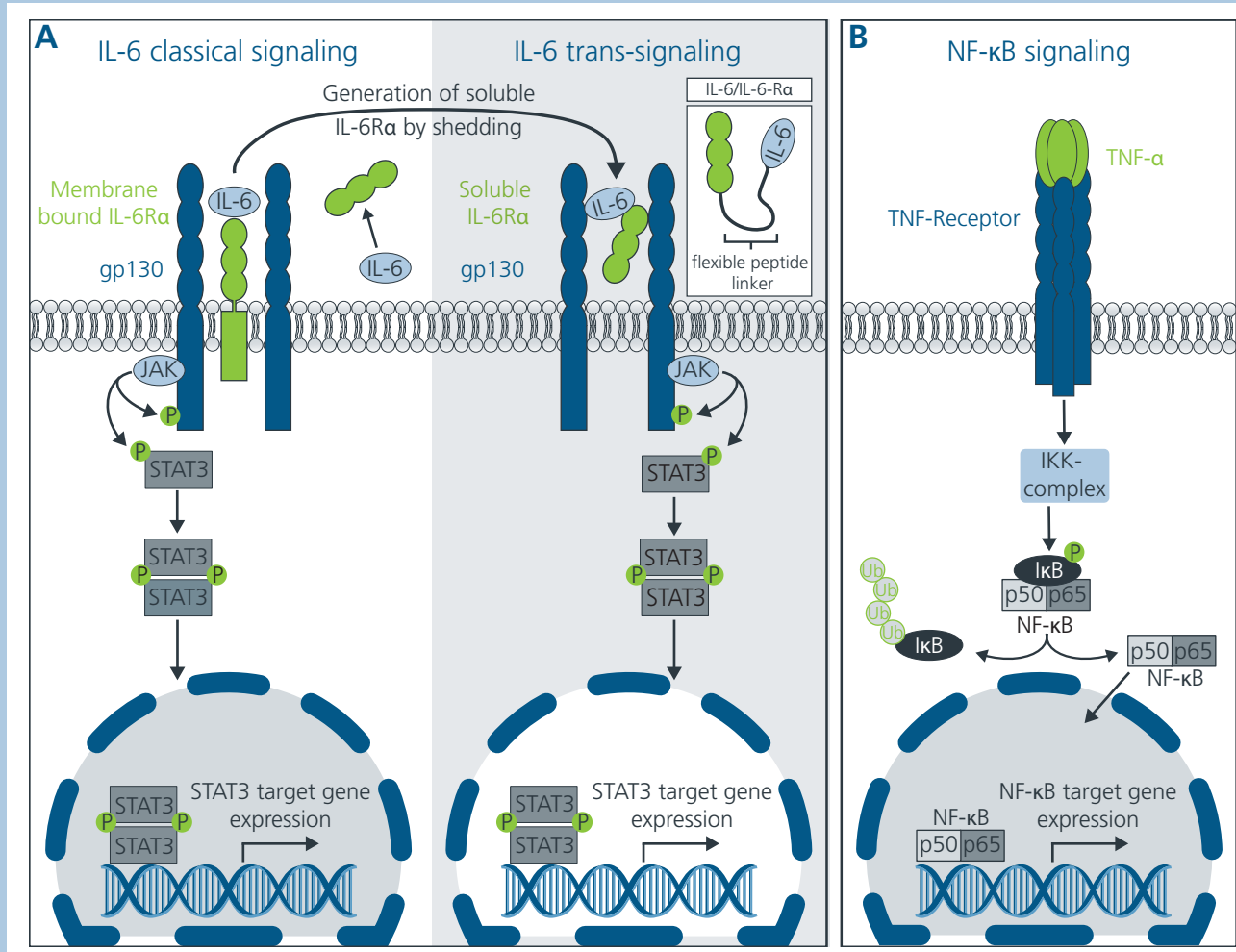


FIG. 1. SCHEMATIC REPRESENTATIONS OF IL-6- AND TNF- $\alpha$ -INDUCED SIGNALING PATHWAYS.

A) Interleukin-6 (IL-6) binds to Glycoprotein 130 (gp130) when it is in a complex with its membrane-bound or soluble receptor, which in turn induces Janus kinase (JAK) dependent phosphorylation of Signal transducer and activator of transcription 3 (STAT3). STAT3 translocates to the nucleus, where it regulates the expression of target genes. Here we used a recombinant Human IL-6/Interleukin-6 receptor  $\alpha$  (IL-6Ra) Protein Chimera to induce the IL-6 signaling pathway. B) Binding of tumor necrosis factor- $\alpha$  (TNF- $\alpha$ ) to its receptor activates the I $\kappa$ B kinase (IKK) complex, which phosphorylates I $\kappa$ B and leads to its ubiquitination and degradation by the proteasome. This liberates nuclear factor 'k-light-chain-enhancer' of activated B-cells (NF- $\kappa$ B) and enables its translocation into the nucleus where it regulates the expression of target genes.

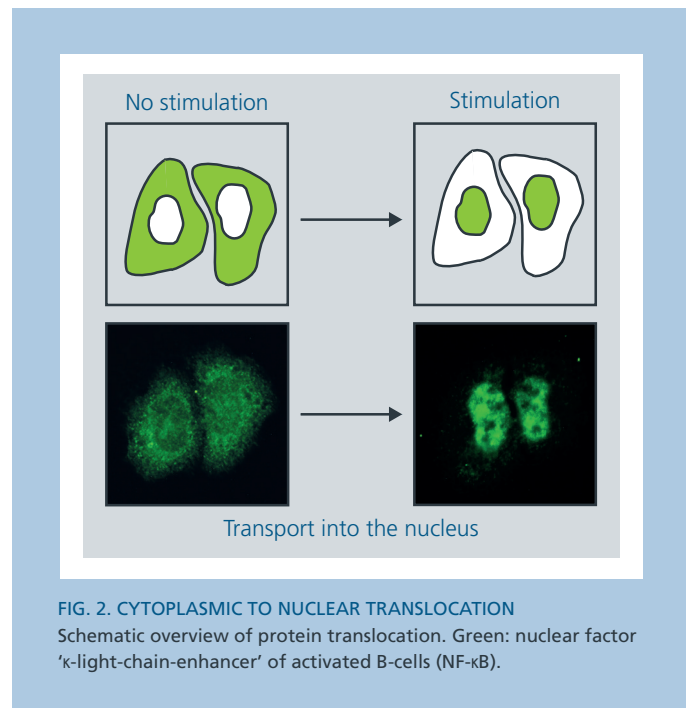
the cytosol and nucleus: signal transducer and activator of transcription 3 (STAT3) and nuclear factor  $\kappa$ -light-chain-enhancer of activated B cells (NF- $\kappa$ B).

STAT3 belongs to a family of transcription factors that controls the expression of genes involved in cellular signaling pathways like cell survival, proliferation, differentiation and immune response. The most potent activators of STAT3 are cytokines of the Interleukin-6 (IL-6) family. There are two IL-6 signaling pathways that exist in cells, IL-6 classical signaling and trans-signaling (Fig. 1A)[4]. In classical signaling, IL-6 binds to its membrane-bound receptor  $\alpha$  (IL-6R $\alpha$ ), and then the complex of IL-6 and IL-6R $\alpha$  associates with the Glycoprotein 130 (gp130). In trans-signaling, IL-6 binds to a soluble form of its receptor  $\alpha$  (sIL-6R $\alpha$ ), generated by alternative splicing or proteolytic cleavage of the membrane-bound form, following binding of the IL-6/sIL-6R $\alpha$  complex to gp130. Trans-signaling via sIL-6R $\alpha$  can occur in any cell in the body since all cells express gp130, while classical signaling is restricted to the membrane-bound form of the IL-6R $\alpha$ , which is only present on certain leukocytes and hepatocytes. The complex of IL-6 and IL-6R $\alpha$  is necessary for gp130 activation. gp130 initiates intracellular signaling of the JAK (Janus kinase)-STAT pathway, the mitogen-activated protein kinase (MAPK) cascade, and the phosphatidylinositide-3-kinase (PI3K) cascade [5]. While IL-6 trans-signaling is associated with inflammatory diseases and inflammation-associated cancer, IL-6 classical signaling through the membrane-bound receptor mediates protective and regenerative functions [4], [5]. Translocation of STAT3 between cytosol and nucleus is initiated by IL-6/sIL-6R $\alpha$ /gp130-dependent JAK activation. JAK phosphorylates STAT3 leading to its dimerization and movement to the nucleus, where it regulates target gene expression (Fig. 1A). In order to induce the IL-6/gp130/STAT3 signaling pathway, here we used recombinant Human IL-6/IL-6R $\alpha$  Protein Chimera, which is an engineered version of the naturally occurring cytokine IL-6 and sIL-6R $\alpha$  [4]. This modified cytokine is designed to have increased potency and specificity in activating cellular signaling pathways. Another prominent transcription factor that upon its activation translocates to the nucleus is NF- $\kappa$ B. Proteins of the NF- $\kappa$ B transcription factor family form homo- and heterodimers with each other, of those the most abundant complex consists of p50 and

## MATERIAL

### Cell Culture and Treatment

- A549 (adherent lung cancer cells)
- HT29 (adherent colon cancer cells)
- RPMI 1640 medium supplemented with 10 % (v/v) FCS, 1 % (v/v) L-Glutamine, 1 % (v/v) Sodium Pyruvate
- Trypsin 0.05 %/EDTA 0.02 % in PBS
- Trypan Blue
- Recombinant Human IL-6/IL-6R $\alpha$  Protein Chimera (Bio-Techne GmbH, 8954-SR)
- TNF- $\alpha$  (like e.g. Peprotech, 300-01A)



p65 subunits [6]. The protein is present in almost all cell types and is a crucial regulator of many physiological and pathophysiological processes, including the control of innate and adaptive immune responses, inflammation, and cancer progression. In resting cells, NF- $\kappa$ B dimers are kept inactive in the cytoplasm by the inhibitory protein I $\kappa$ B (inhibitor of NF- $\kappa$ B). A potent activator of NF- $\kappa$ B is the cytokine tumor necrosis factor- $\alpha$  (TNF- $\alpha$ ), which plays a role in the cellular response to infection or inflammation. Upon binding to its receptor, TNF- $\alpha$  activates the I $\kappa$ B kinase complex (IKK) consisting of two catalytic subunits, IKK $\alpha$  and IKK $\beta$ , and a regulatory subunit called NEMO (NF- $\kappa$ B essential modulator) [6], [7]. IKK induces the phosphorylation, ubiquitination, and proteasomal degradation of I $\kappa$ B. The release of NF- $\kappa$ B from its inhibitor I $\kappa$ B induces its translocation to the nucleus, where it regulates the expression of target genes (Fig. 1B).

Utilizing these signaling pathways as two models (Fig. 2), we developed an image analysis application within our YT-SOFTWARE®.

### Immunofluorescence Staining

- 96 well black glass bottom plate (e.g. Greiner, 655891)
- Poly-D-Lysine (Gibco, A38904-01)
- Fixation Buffer (BioLegend, 420801)
- 100 % Methanol (v/v)
- 3 % (w/v) Bovine Serum Albumin/0.1 % (v/v) Tween 20 in PBS
- PBS (like e.g. gibco, 10010023)

### Imaging and Analysis

- SYNENTEC's imaging device (here NYONE® Scientific and CELLAVISTA® 4K)

## METHODS

### Cell culture and cell counting

Human A549 lung cancer cells and HT29 colon cancer cells were cultured in RPMI 1640 medium supplemented with 10 % (v/v) FCS, 1 % (v/v) Sodium Pyruvate, and 1 % (v/v) L-Glutamine under standardized cell culture conditions (37 °C, 5 % CO<sub>2</sub>, humidified atmosphere). Cells were routinely passaged at 70–80 % confluence. Therefore, cells were detached with Trypsin, and counted using SYNENTEC's **Trypan Blue** application. The appropriate cell number was calculated based on the *viable cell density*.

### Immunofluorescence staining

In order to be able to perform translocation experiments with multiple samples in parallel and to simplify handling, we used 96 well plates. To obtain images with the best quality, we used black plates with a glass bottom. These are highly recommended when conducting high-content measurements with 20x or 40x magnification.

96 well glass bottom plates were coated with 50 µL Poly-D-Lysine according to the manufacturer's protocol before cell seeding. The following numbers of cells were seeded in the pre-coated wells using a multistep pipette (200 µL/well): 2,000 A549 cells/well for IL-6/IL-6R $\alpha$  treatment and 4,000 cells/well for TNF- $\alpha$  treatment; 3,000 HT29 cells/well for IL-6/IL-6R $\alpha$  treatment, and 5,000 cells/well for TNF- $\alpha$  treatment. After two days, FCS was reduced for TNF- $\alpha$  treatment to 0.5 % (v/v). On day three after seeding, cells were stimulated with 50 ng/mL IL-6/IL-6R $\alpha$  or 100 ng/mL TNF- $\alpha$  for 15 min, 30 min, 45 min, and 60 min. In parallel, the medium was exchanged as a control for each time point. Thereafter, cells were immediately fixed with cold 4 % paraformaldehyde/PBS (15 min). After washing three times with PBS (100 µL/well, 5 min), cells were permeabilized with ice-cold 100 % methanol (50 µL/well, 10 min, at -20 °C), followed by another washing step (2x, 100 µL/well PBS, 5 min). In order to reduce unspecific antibody binding, cells were incubated with 3 % BSA in PBS and 0.1 % Tween 20 (50 µL/well) for 45 min at room temperature. Afterward, primary antibodies (mouse anti-STAT3 (81,88 ng/mL) or rabbit anti-NF- $\kappa$ B (2 µg/mL) diluted in blocking solution were added and incubated overnight (50 µL/well, 4 °C). Subsequently, cells were washed twice with PBS (100 µL/well, 5 min) and incubated with secondary fluorochrome-conjugated antibodies (anti-mouse Alexa Fluor 488 (2 µg/mL) or anti-rabbit Alexa Fluor 488 (2 µg/mL)) diluted in blocking solution at room temperature in the dark (50 µL/well, 1 h). After two washes (100 µL/well PBS, 5 min), nuclei were stained by Hoechst 33342 (2.5 µg/mL) and the cytoplasm by HCS CellMask™ deep red (2 µg/mL) diluted in PBS (50 µL/well, 20 min). Cells were washed twice (100 µL/well PBS, 5 min) and finally, 200 µL PBS were added to the wells. Immunofluorescence stainings were imaged using NYONE® Scientific (20x magnification) and CELLAVISTA® 4K (40x magnification) and quantified using the **Translocation (1F)** image analysis application of YT-SOFTWARE® (Fig. 3).

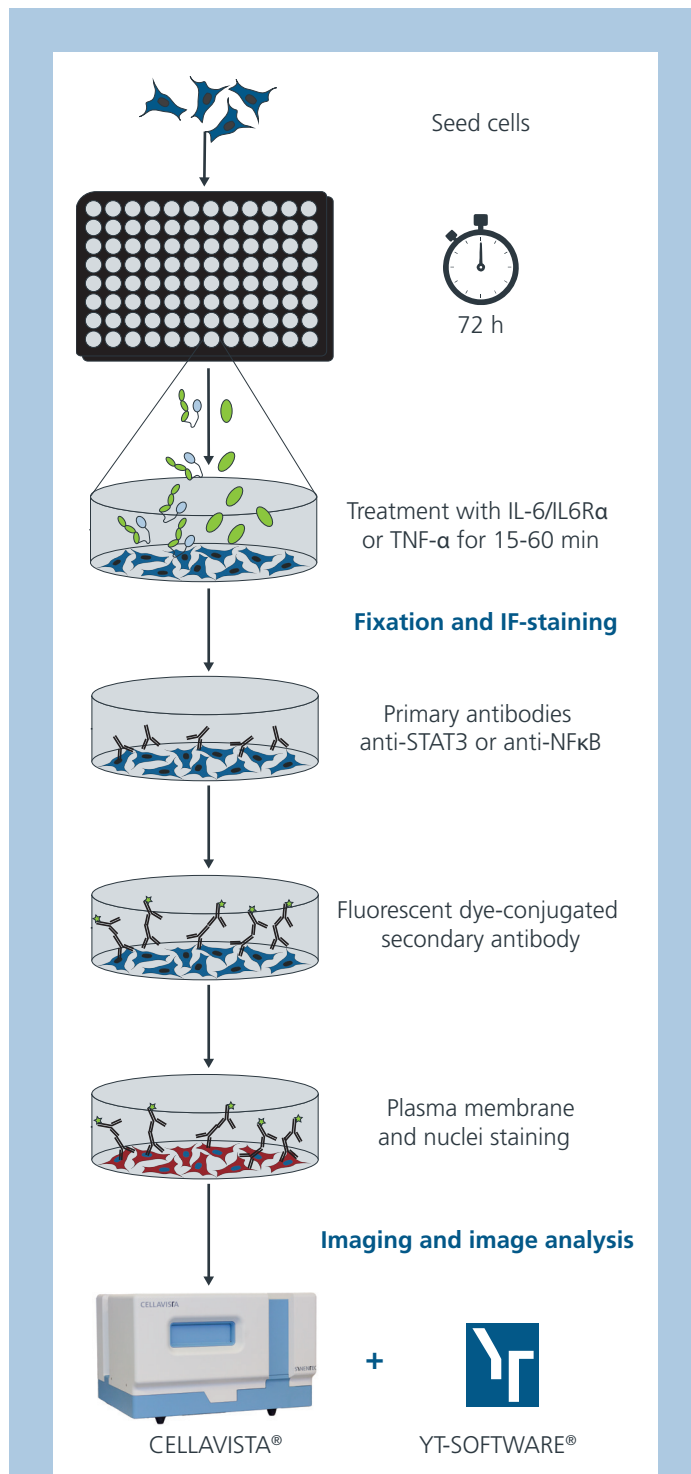


FIG. 3. OVERVIEW OF THE EXPERIMENTAL SETUP

Cells were seeded in a 96 well glass bottom plate. After 72 h, cells were treated with Interleukin-6/Interleukin-6 receptor  $\alpha$  (IL-6/IL-6R $\alpha$ ) or tumor necrosis factor- $\alpha$  (TNF- $\alpha$ ) for 15–60 min. Afterward, indirect immunofluorescence staining was performed using anti-STAT3 (Signal transducer and activator of transcription 3) or anti-NF- $\kappa$ B (nuclear factor 'k-light-chain-enhancer' of activated B-cells) primary antibodies and Alexa Fluor 488-conjugated secondary antibodies. For cell segmentation, cells were stained with Hoechst 33342 and HCS CellMask™. Finally, stainings were imaged and analyzed using CELLAVISTA® and YT-SOFTWARE®.

TABLE 1: ANTIBODIES AND STAINS

Name	Source/Isotype	Manufacturer	Catalog #	Stock Concentration	Final Concentration
STAT3 (124H6)	Mouse/IgG2a	Cell Signaling	9139S	131 µg/mL	81.88 ng/mL
NF-κB p65	Rabbit/IgG	Santa Cruz	sc-109	100 µg/mL	2 µg/mL
Anti-Rabbit Alexa Fluor™ 488	Goat/IgG	Invitrogen	A-11008	2 mg/mL	2 µg/mL
Anti-Mouse Alexa Fluor™ 488	Goat/IgG	Invitrogen	A-11001	2 mg/mL	2 µg/mL
HCS CellMask™ Deep Red		Invitrogen	H32721	10 mg/mL	2 µg/mL
Hoechst 33342		Invitrogen	H1399	5 mg/mL	2.5 µg/mL

## RESULTS & DISCUSSION

### Development of a Protein Translocation Application

Image processing was developed on immunofluorescence stainings of the cytosol and nucleus. First, based on Hoechst 33342 staining, a nuclear mask was generated (Fig. 4, green circle). In the second step, the mask of the nuclei was extended referring to the HCS CellMask™ signal to determine the area of the whole cell (Fig. 4, violet border). Third, the nuclear mask was subtracted from the whole cell to identify the cytoplasm. This enabled the quantification of the *average fluorescence intensity* of the nuclei and cytoplasm and the calculation of the *translocation ratio*, which is the ratio of the average nuclei intensity to the average cytoplasmic intensity (nucleus/cytoplasm) of the protein of interest (here STAT3 and NF-κB). Cells counted positive for nuclear translocation were marked with an orange circle around the nucleus. Within our readily accessible **Translocation (1F)** software application, these procedural steps are pre-configured. Consequently, masks and values can be readily acquired through the 'process image' button.

### Analysis of STAT3 translocation in HT29 cells

To test our newly developed application, we analyzed the translocation of STAT3. Therefore, HT29 colon carcinoma cells were treated with recombinant IL-6/IL-6Rα for several time points and immunofluorescence stainings were performed afterward. Staining of STAT3 in untreated cells showed a homogenous protein distribution across the whole cell (Fig. 5A). In contrast, after treatment with IL-6/IL-6Rα, the fluorescence signal of STAT3 was clearly increased in the nucleus of HT29 cells compared to the cytosolic region. Although phosphorylation of STAT3 induces its movement to the nucleus, it has also been described that its nuclear import can take place independently of the phosphorylation status [8]. Moreover, in numerous cancer cells derived from various tumor entities, STAT3 is constitutively activated playing a key factor in oncogenesis, metastasis, and recurrence [9]. Since we used an

antibody that is specific for total STAT3, we could not distinguish if the detected protein was phosphorylated or not. This might explain the nuclear presence of STAT3 even in untreated cells.

Results obtained from image analysis of the immunofluorescence stainings using the **Translocation (1F)** application of YT-SOFTWARE® supported our observations. After IL-6/IL-6Rα treatment, the average STAT3 fluorescence intensity in the cytosolic region was decreased, while a concurrent increase was evident in the nuclear region (Fig. 5B). Notably, the translocation ratio rose from approximately 1.8 to 7.0 within 30 minutes after treatment. As time progressed, the signal began to decline again, reaching 3.4 after 60 minutes post-treatment (Fig. 5C). Similar results could be obtained in A549 lung carcinoma cells. Upon treatment of A549 cells with IL-6/IL-6Rα, STAT3 translocation increased already 15 min after treatment (2.6 to 9.1), reaching a peak after 30 min (11.6), until it slowly dropped down again after 45 min (10.4) and 60 min (6.2; data not shown). These findings underscore the dynamic nature of STAT3 translocation, enabling a rapid signal transduction and cellular response to external factors.

### Analysis of NF-κB translocation in A549 cells

In order to test our newly developed image analysis application on another cell line and another protein, we induced NF-κB trafficking over a time course of 15 to 60 minutes by TNF-α in A549 lung carcinoma cells and performed immunofluorescence stainings afterward. In untreated cells, only very faint NF-κB was detectable in the nuclei (Fig. 6A). In contrast, already 15 minutes post-treatment, the NF-κB fluorescence signal clearly increased in the nuclear region. Simultaneously, the fluorescence signal in the cytoplasmic region diminished (Fig. 6A). Results obtained from image analysis using the **Translocation (1F)** application of YT-SOFTWARE® confirmed these observations. After treatment with TNF-α, the *average fluorescence intensity* of NF-κB decreased in the



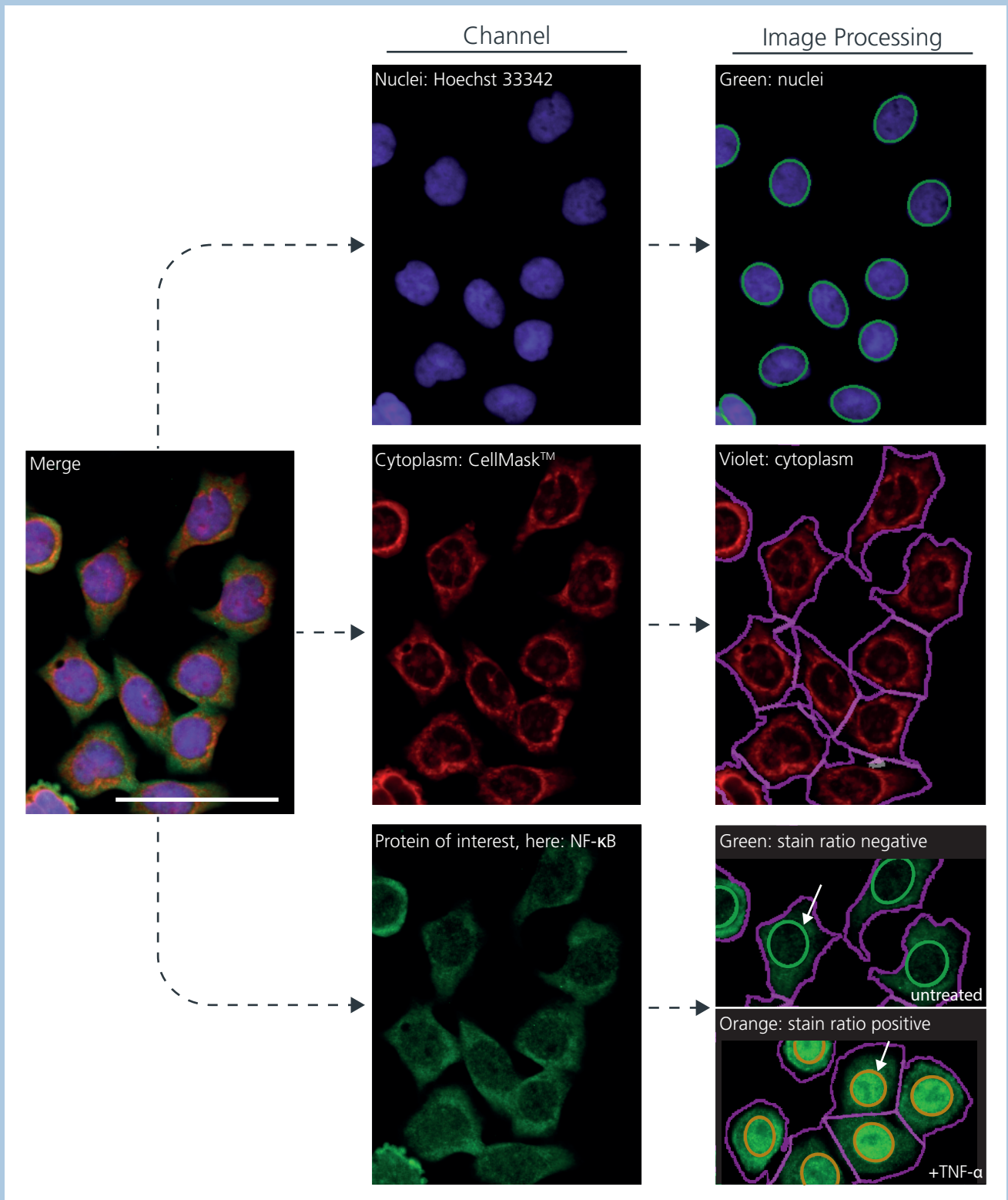
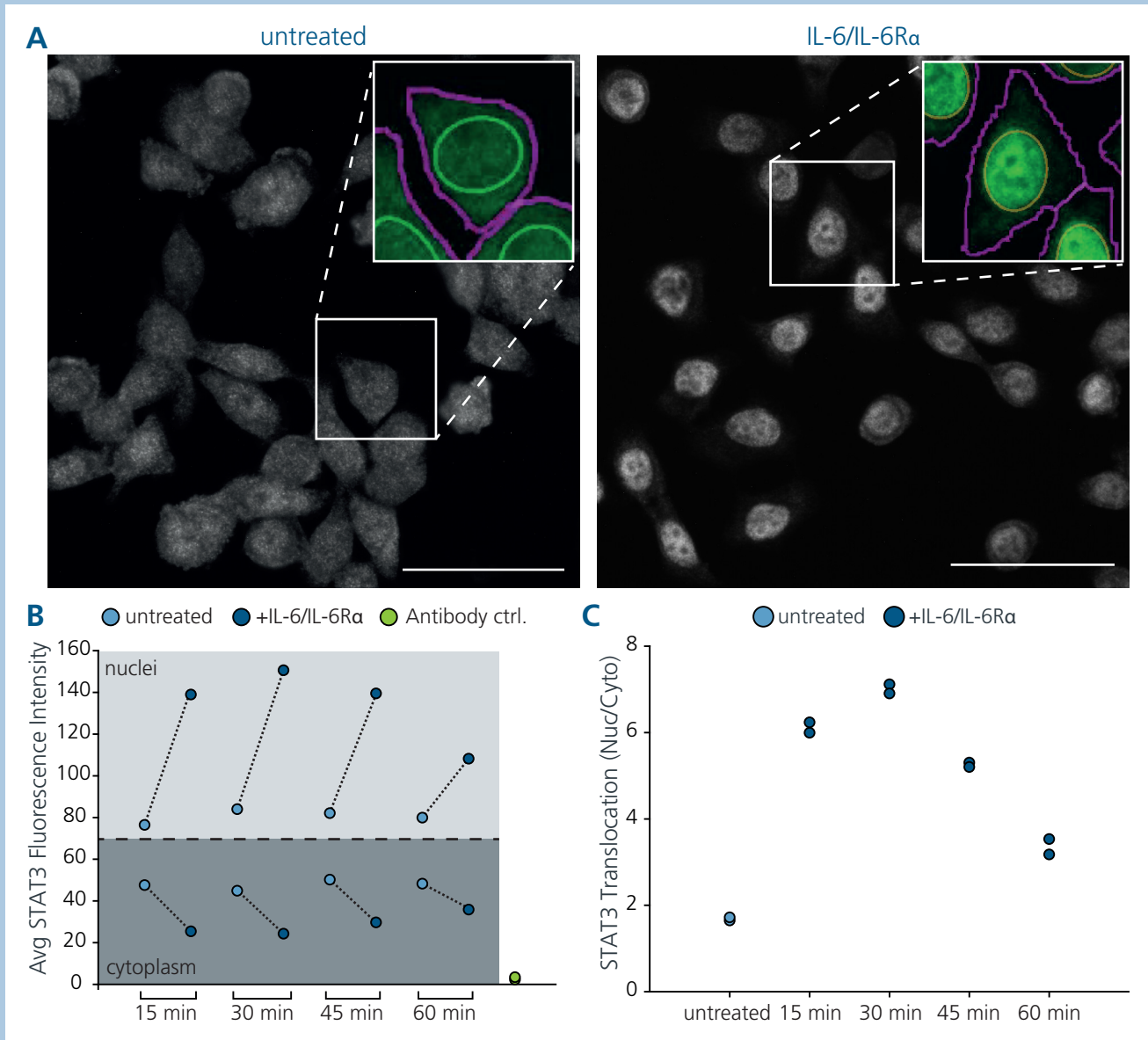


FIG. 4. THE TRANSLOCATION (1F) IMAGE ANALYSIS APPLICATION SEGMENTS CELLS INTO NUCLEI AND CYTOPLASM AND CALCULATES THE TRANSLOCATION RATION OF A PROTEIN OF INTEREST

Hoechst-stained nuclei are marked in green, the cytoplasm is outlined in purple, and cells that are positive for nuclear translocation (here: +TNF- $\alpha$ , tumor necrosis factor-alpha; staining: NF- $\kappa$ B, nuclear factor 'k-light-chain-enhancer' of activated B-cells) are highlighted with an orange circle around the nuclei. Scale bar: 50  $\mu$ m.



**FIG. 5. IL-6/IL-6R $\alpha$  INDUCES STAT3 TRANSLOCATION**

HT29 cells were seeded in a 96 well microplate, treated with 50 ng/mL Interleukin-6/Interleukin-6 receptor  $\alpha$  (IL-6/IL-6R $\alpha$ ) for 15 to 60 min, fixed, and stained using anti-STAT3 (Signal transducer and activator of transcription 3) antibody and anti-mouse Alexa Fluor 488 secondary antibody. A) Shown are representative immunofluorescence pictures of untreated (control) and treated (30 min) HT29 cells taken with CELLAVISTA<sup>®</sup> 4K at 40x magnification. Images were analyzed using the **Translocation (1F)** application of YT-SOFTWARE<sup>®</sup>. B) The average STAT3 fluorescence intensities of the cytosolic and nuclear regions were determined (data are presented as mean of 1 experiment, performed in 2 technical replicates). C) The translocation ratio of STAT3 was calculated (data are presented of 1 experiment, performed in 2 technical replicates). Scale bar 50  $\mu$ m.

cytoplasmic and increased in the nuclear region (Fig. 6B). This effect was independent of the treatment duration. The automatically calculated *translocation ratio* increased from approximately 2 in untreated cells to around 4 in treated cells, varying only slightly between the different treatment durations (Fig. 6C). Similar results could be obtained by performing the same experimental setup with HT29 cells. Here, after stimulation with TNF- $\alpha$  for 15 min the *average fluorescence intensity* of NF- $\kappa$ B was also clearly enhanced in the nucleus and lasted at a relatively constant level over 60 min

(data not shown).

In case of untreated cells one would expect a *translocation ratio* of 1 or lower, since the cytoplasmic fluorescence intensity should be higher than the nuclear intensity in these cells. However, we obtained higher values in both experimental setups. This discrepancy can be explained by a fluorescence gradient that spans from the cellular center to its periphery, which decreases the cytoplasmic *average fluorescence intensity*.

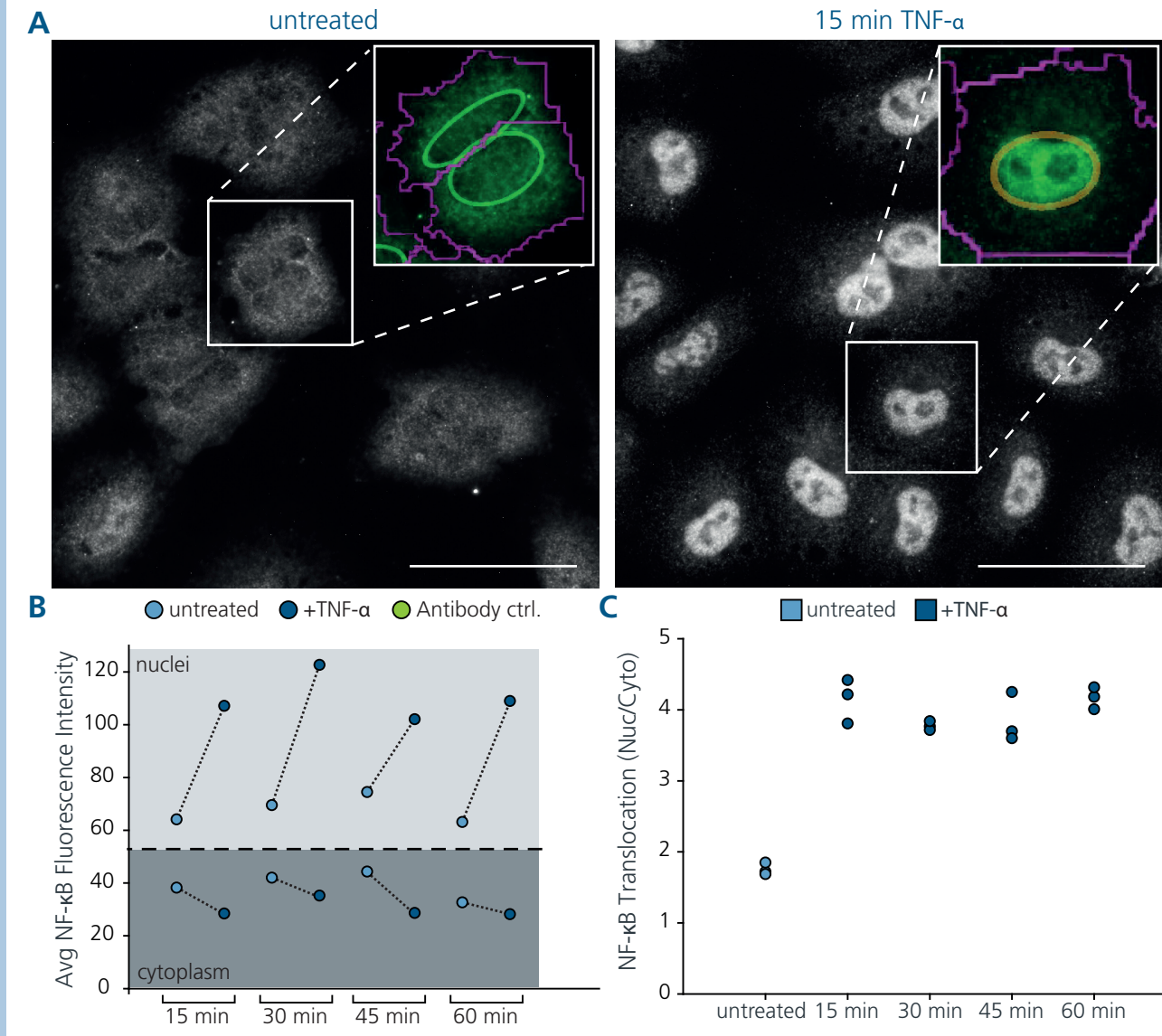


**FIG. 6. TNF- $\alpha$  INDUCES NF- $\kappa$ B TRANSLOCATION**

A549 cells were seeded in a 96 well microplate, treated with 100 ng/mL tumor necrosis factor- $\alpha$  (TNF- $\alpha$ ) for 15 to 60 min, fixed and stained using anti-NF- $\kappa$ B (nuclear factor 'k-light-chain-enhancer' of activated B-cells) antibody and anti-rabbit Alexa Fluor 488 secondary antibody. A) Shown are representative immunofluorescence pictures of untreated and treated (15 min) A549 cells taken with CELLAVISTA 4K at 40x magnification. Images were analyzed using the **Translocation (1F)** application of YT-SOFTWARE<sup>®</sup>. B) The average NF- $\kappa$ B fluorescence intensities of cytosolic and nuclear regions were quantified (data are presented as mean of 1 experiment, performed in 3 technical replicates). C) The translocation ratio was calculated (data are presented of 1 experiment, performed in 3 technical replicates). Scale bar 50  $\mu$ m.

## CONCLUSION

Our automated imagers NYONE<sup>®</sup> and CELLAVISTA<sup>®</sup> combined with YT-SOFTWARE<sup>®</sup> provide a valuable tool to detect and quantify cytosolic to nuclear protein translocation. The image analysis application **Translocation (1F)** enables an easy and fast quantification of the *average fluorescence intensities* of the cytoplasmic and nuclear regions and the *translocation ratio* is automatically calculated. By performing translocation assays of two different proteins in two cancer cell lines, we showed that we

established a robust protocol to study protein trafficking. The assay is suitable for high-throughput screening, due to its compatibility with multiwell plate formats. Because the cytoplasm as well as the nuclei are stained and segmented, several features can be extracted (nuclei intensity, cytoplasmic intensity, translocation ratio, nucleus size, nuclei count). Thus, it can be used in high-content screening applications.



## References

- [1] H. J. Kim and J. P. Taylor, "Lost in Transportation: Nucleocytoplasmic Transport Defects in ALS and Other Neurodegenerative Diseases," *Neuron*, vol. 96, no. 2, pp. 285–297, Oct. 2017. doi: 10.1016/j.neuron.2017.07.029.
- [2] X. Wu et al., "Targeting protein modifications in metabolic diseases: molecular mechanisms and targeted therapies," *Signal Transduction and Targeted Therapy*, vol. 8, no. 220, May 2023. doi: 10.1038/s41392-023-01439-y.
- [3] E. Gutiérrez-Galindo, Z. H. Yilmaz, and A. Hausser, "Membrane trafficking in breast cancer progression: protein kinase D comes into play," *Frontiers in Cell and Developmental Biology*, vol. 11, May 2023. doi: 10.3389/fcell.2023.1173387.
- [4] S. Rose-John, "Interleukin-6 signalling in health and disease," *F1000Res*, vol. 9, Aug. 2020, doi: 10.12688/f1000research.26058.1.
- [5] F. Schaper and S. Rose-John, "Interleukin-6: Biology, signaling and strategies of blockade," *Cytokine and Growth Factor Reviews*, vol. 26, no. 5, pp. 475–487, Oct. 2015. doi: 10.1016/j.cytogfr.2015.07.004.
- [6] A. Oeckinghaus and S. Ghosh, "The NF-kappaB family of transcription factors and its regulation.," *Cold Spring Harbor perspectives in biology*, vol. 1, no. 4., Sep. 2009. doi: 10.1101/cshperspect.a000034.
- [7] J. H. Shi and S. C. Sun, "Tumor necrosis factor receptor-associated factor regulation of nuclear factor κB and mitogen-activated protein kinase pathways," *Frontiers in Immunology*, vol. 9, Aug. 2018. doi: 10.3389/fimmu.2018.01849.
- [8] L. Liu, K. M. McBride, and N. C. Reich, "STAT3 nuclear import is independent of tyrosine phosphorylation and mediated by importin-3," *PNAS*, vol. 102, no. 23, May 2005, doi: 10.1073/pnas.0501643102.
- [9] H. Lee, A. J. Jeong, and S. K. Ye, "Highlighted STAT3 as a potential drug target for cancer therapy," *BMB Reports*, vol. 52, no. 7, pp. 415–423, Jul. 2019. doi: 10.5483/BMBRep.2019.52.7.152.

## Acknowledgement

We thank the Institute for Experimental Cancer Research, especially Prof. Susanne Sebens and Prof. Anna Trauzold, for outstanding support, fruitful discussions and a great working atmosphere during this cooperation.



Institut  
für  
Experimentelle  
Tumor-  
forschung

THIS APPLICATION IS COMPATIBLE WITH ALL OUR DEVICES AND IS IMPLEMENTED IN YT-SOFTWARE®. AN AUTOMATED LENS CHANGER IS NOT MANDATORY.



CELLAVISTA® 4K



NYONE®

published 10/2023